RSC Advances

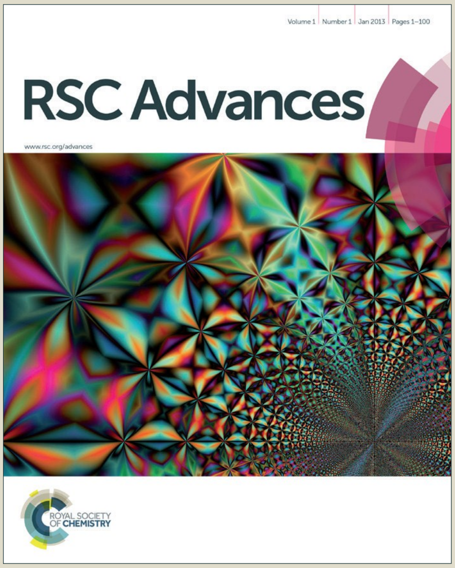

ROYAL SOCIETY OF CHEMISTRY

www.rsc.org/advances

Synthesis and characterization of polyurethane/ poly vinyl pyridine composite membranes for desulfurization of gasoline

Mohammad Rosta[1], Azam Marjani[*,1], Mehdi Ghadiri[2]

[1]Islamic Azad University, Arak Branch, Department of Chemistry, Arak, Iran

[2]Young Researchers and Elite Club, South Tehran Branch, Islamic Azad University, Tehran, Iran

[*] Corresponding author: a-marjani@iau-arak.ac.ir

Tel.: +98 8614132451, Fax: +98 861 4132459

Abstract

Polyurethane/ poly vinyl pyridine (PU/PVP) composite membranes were prepared applicable to desulfurization of gasoline. The prepared composite membranes were characterized using scanning electron microscopy to ensure the fine dispersion of PVP in PU polymer and swelling test was conducted to determine the potential applicability of composite membranes used in desulphurization of gasoline. Hydrophilicity of the synthesized membranes were analyzed through measuring contact angle, and a considerable enhancement in the hydrophilicity of mixed matrix membranes was observed compared to the pure PU membranes. The performance membranes were evaluated in pervaporation (PV) desulfurization of gasoline at different operating conditions. Influence of operational parameters including feed flow rate, concentration of sulfur in feed stream, and feed temperature on the pervaporation performance of prepared composite membranes were studied. Permeation flux increased with increasing feed flow rate and operating temperature while it remained almost constant with enhancement of sulfur content in the feed. On the other hand, sulfur enrichment factor decreased with increasing sulfur content in the feed stream. In addition, a novel mathematical model was developed to simulate the pervaporation system. The model was on the basis of solving the continuity equation for sulfur in the feed side and membrane.

Keywords: Membrane Processes; Synthesis; Desulfurization; Pervaporation; Modeling;

1- Introduction

There are various types of sulfur compounds in gasoline such as sulfides, thiols, and mercaptans. These sulfur compounds are converted into sulfur dioxide (SO_2) during combustion of gasoline in automobile engines. In addition, most refineries have to process high sulfur content in crude oil due to lack of availability of lighter, low sulfur crude. Also, the environmental regulatory restricts on sulfur emissions are continually being lowered; therefore, technical development for deep desulfurization of gasoline to prevent adverse effects of sulfur compounds in fuels is urgent and attracting increasing attention[1-4].

A number of remedies have been suggested to decrease the content of sulfur compounds in gasoline; however none of them have been proven to be useful and efficient at industrial scale. Hydro-treating of the feed is one of them most important processes for reduction of sulfur level in gasoline appropriate level. However, installing the required hydro-treating capacity needs a considerable capital expenses and causes the enhancement of operating costs[5-7].

Most separation processes at industrial scale are based on energy-extensive approaches including evaporation, distillation and crystallization. The latter processes will face major issues by increasing energy crisis worldwide. Among the different kinds of separation processes, membrane systems have attracted much attention as an alternative to traditional separation systems. Membrane separation processes have benefits which make them attractive for separation of liquid and gases mixtures. High separation efficiency, no waste streams, low energy and operating expenses, and are suitable for heat-sensitive chemicals[8-10].

Desulfurization of gasoline can be implemented using membrane separation technology. Various membrane technologies are used in separation and purification of liquid including microfiltration (MF), ultrafiltration (UF), reverse osmosis (RO), electrodialysis (ED), and pervaporation (PV). Among the membrane processes, pervaporation has attracted much attention in separation of liquid mixtures due to its unique advantages compared to other ones. Pervaporation provides a low-energy process in desulfurization of gasoline and the main energy is consumed in vacuum section of process[11-19].

Separation of liquid mixtures into its constituents by pervaporation takes place by application of a dense membrane. The transport of species through the membrane is occurred due to differences in chemical potential of components across the membrane. The used membrane in pervaporation could be either polymeric or ceramic depending on the required specifications. The governing separation mechanism in pervaporation is solution-diffusion mechanism[13, 20, 21]. In principle, in pervaporation the transport of molecules through the membrane involves three steps in series: first selective sorption of molecules from feed into the dense membrane, second; diffusion of molecules through the membrane matrix, and third; desorption into the vapor phase at permeate side[22, 23]. Therefore, the transport rate of molecules through the membrane is functions of solubility and diffusivity because the desorption step is fast due to the efficient vacuum at downstream. Industrial applications of PV technology can be mentioned as removal of organic components from aqueous wastes, dehydration of solvents, and separation of organic/organic mixtures[24, 25].

In the recent years, various polymers such as polyurethane, polyimide, PDMS, polyethylene glycol, poly phosphazene, polyvinylidene fluoride, polyhedral oligomeric silsesquioxane, and polysulfon have been used as membrane material for sulfur removal from gasoline [21, 26, 27]. Also, various authors have worked to improve the membranes performance by blending the membrane materials with various filler particles or other polymers, by optimizing the cross linking of polymeric resins or by modifying the membrane via functionalizing them[28-30]. To our knowledge, there have been no reports of pervaporation for removing sulfur compounds from gasoline using PVP/PU composite membranes. So, the aim of this work is synthesis and investigation of PVP/PU composite membranes for removal of sulfur from gasoline in pervaporation system.

In the current work, PVP/PU composite membranes were synthesized for gasoline desulfurization. Membrane characterization was conducted by scanning electron microscopy and swelling test. With the refinery naphtha feed stream, the pervaporation and desulfurization performance of the blend membranes under different conditions were investigated. All these investigations provide helpful suggestions for the newly emerged membrane desulfurization technology. Furthermore, a mathematical model is developed to simulate the pervaporation system. The model is on the basis of solving conservation equations for sulfur in the membrane module.

2- Experimental

2-1- Materials

Polyurethane and poly vinyl pyridine used for preparation of membranes were purchased from Aldrich Company. PU is used in many industrial applications because they show wide mechanical properties from rubber to plastic and resistance to different solutions. Refinery naphtha feed was obtained from Imam Khomeini Refinery (Shazand, Iran). Other chemicals used were of analytical grade reagents and used as received without further purifications.

2-2-Membrane preparation

Polyurethane (PU) was dissolved into *n*-heptane to form a homogenous solution at room temperature. Then poly vinyl pyridine (PVP) was added into the solution under stirring condition. In order to promote the dispersion of polymer particles, the suspension was then sonicated for 5 min. After filtration and degassing, the solution was cast onto a glass plate. Afterward, the cast film was placed in the ambient air for certain period of time and then placed in an oven to evaporate the residual solvent. Finally, the dried membranes were separated from glass surface at room temperature and the homogeneous membrane was obtained. The synthesized membranes have high quality and do not damage during the spreparation. Besides, those have higher resistance towards gasoline. The structure of the synthesized membranes was not change when they were placed in the gasoline for a week.

2-3-Membrane Characterizations

2-3-1- Scanning electron microscopy (SEM)

Scanning electron micrographs of composite membranes were performed on a Philips XL-30M scanning electron microscope (SEM) instrument. All specimens were coated with a thin layer of gold prior to analysis to prevent charging.

2-3-2- Contact angle measurement

The hydrophilicity of pure and mixed matrix membranes was evaluated by measuring the contact angle formed between the membrane surface and water drop. The contact angle was measured by using an optical contact angle goniometer from Dataphysics Instruments (OCA20) at room temperature which uses static sessile drop method for measuring contact angle. All contact angle measurements were conducted via 5 μL of deionized water. The contact angle was measured at two random locations for each sample and the average was reported.

2-4- Pervaporation experiments

To assess the performance of synthesized composite membranes in desulfurization of gasoline, an experimental pervaporation setup was installed as illustrated in Fig. 1. Effect of feed concentration and temperature on mass flux and enrichment factor of sulfur was investigated. Feed solutions at different concentrations ranging from 220-800 ppm were prepared and fed to the membrane module at a constant flow rate. The temperature of feed stream was adjusted between 300 and 360 K using a constant-temperature heat bath. Pervaporation experiments were conducted in cross-flow mode. The synthesized composite membrane was placed inside the module with an effective area of 13.852 cm^2. A rubber O-ring was used to provide a pressure seal between the module and the blend membrane. Pressure at permeate side was maintained at 0.3 bar by an oil-sealed vacuum pump (JB, USA). Permeate vapors were condensed and collected in a cold trap (glass vessel) kept inside a liquid nitrogen reservoir. The permeate samples collected in the glass vessel were analyzed after weighting, using gas chromatography method. Total permeation flux (J) was determined using equation (1):

$$J = \frac{m}{A.t} \tag{1}$$

where m (kg) is total mass of permeate collected through effective area of the composite membrane A (m^2) during the time interval t (h). In order to investigate the reproducibility of the experimental results, all experiments are carried out two times.

The enrichment factor is qualitative criterion for evaluation of membrane separation performance. It is can be written as follow:

$$E = \frac{C_{s,p}}{C_{s,f}} \tag{2}$$

where $C_{s,f}$ (ppm) and $C_{s,p}$ (ppm) are total sulfur content in feed and permeate streams.

Fig. 1: Experimental setup used for pervaporation desulphurization of gasoline.

2-5- Mathematical modeling

To prognosticate the separation performance of membranes, a 2D mathematical model is developed in this study. The model is developed on the basis of solving conservation equations for sulfur in the feed and membrane. Several researcher has been used from this model to simulation of membrane processes[31-34]. Fig. 2 depicts the domain used in the modeling of system.

Fig. 2: Model domain used in the simulation.

As shown, feed solution containing sulfur and gasoline is passed in the feed side, the sulfur is transferred against the membrane because of concentration difference and then diffuses through the dense membrane, and finally sulfur desorbs into the permeate side. Thus, the model domain is divided into three sub-domains, i.e. feed, membrane, and permeate.

The main equation that describes the transfer of sulfur from gasoline to permeate side is continuity equation. This equation is derived from mass balance of sulfur within an element. The differential form of continuity equation for sulfur is given as follow[35]:

$$\frac{\partial C_s}{\partial t} + \nabla.\left(-D_s \nabla C_s + C_s V\right) = R_s \qquad (2)$$

where C_s, D_s, V, R_s denote sulfur concentration (mol/m^3), diffusivity of sulfur (m^2/s), velocity vector (m/s), and chemical reaction (mol/m^3.s) respectively. It should be mentioned that the chemical reaction is not considered in the simulation.

Eq. 2 is developed for feed and membrane compartments. To solve Eq. 2 for feed side, velocity distribution is required. The velocity distribution in the feed side can be calculated via solving the Navier-Stokes equations which may be written as follows[36, 37 35]:

$$\begin{aligned} &-\nabla.\mu\left(\nabla V_y + (\nabla V_y)^T\right) + \rho\left(V_y.\nabla\right)V_y + \nabla p = F \\ &\nabla V_y = 0 \end{aligned} \qquad (3)$$

where η denotes the dynamic viscosity (kg/m·s), Vy the velocity vector in y direction (m/s), ρ the density of the fluid (kg/m^3), p the pressure (Pa) and F is a body force term (N). Boundary conditions for equations can be categorized according to their domains which are shown in Table 1.

The equations of model used with the boundary conditions were solved numerically via COMSOL Multiphysics software. A system with the specifications of RAM 4.00 GB (2.98 GB usable) and Intel® Core™ i5CPU M 480 @ 2.67GHz and 64-bit operating system was used to solve the equations of model. The accuracy of numerical procedure was proved in the previous publications [31, 36, 38-45].

Table 1: Boundary conditions for momentum and mass transfer equations

3- Results and discussion

3-1- SEM and contact angle characterization

The synthesized membranes were characterized using scanning electron microscopy (SEM) to observe the dispersion of PVP inside PU polymer matrix. Fig.3 illustrates SEM images of synthesized membranes at various PVP loadings ranging from PVP/PU ratio of 0 to 1. As it can be seen, From Fig. 3a no porous structure is visible on the surface of dense PU membrane. Increasing PVP loading results in the enhancement of particles distribution in PU polymer matrix which in turn reduces the separation performance of synthesized membranes. It is also seen that increasing PVP content would result in agglomeration of PVP in the polymer. Agglomeration of particles inside a polymer matrix is not favorable in synthesis of high-quality membranes. The latter could results in increasing permeation, but separation factor decreases drastically. Moreover, at high PVP loading, agglomerates with the size of 3 microns can be observed.

Fig. 4 presents the measured contact angle values for pure PU and mixed matrix membranes (content of PVP). Compared with pure PU membrane, the contact angle of mixed matrix membranes decreased distinctly, indicating that a more hydrophilic membrane has been synthesized. In general, it was considered that the materials with lower water contact angle have a better hydrophilic property [46], so, the mixed matrix membranes exhibited a more hydrophilicity in comparison with that of pure PU membranes. In addition, surface tension of pure PU and mixed matrix membranes is shown in Table 2. According to Table 2, increasing content of PVP in the mixed matrix membranes decreases surface tension. The latter means the hydrophilicity of mixed matrix membrane increases with enhancement of PVP content in the mixed matrix membranes.

Fig. 3: SEM images of synthesized composite membranes at different PVP loadings. a: pure PU; b: PVP/PU=0.2; c: PVP/PU=0.4; d: PVP/PU=0.6; e: PVP/PU=0.8; f: PVP/PU=1.

Fig 4: Contact angles of 0% PVP, 40% PVP, 80% PVP.

Table 2: Surface tension of 0% PVP, 40% PVP, 80% PVP.

3-2- Effect of feed temperature

The enrichment factor and mass transfer flux as function of feed temperature are shown in Fig. 5. The range of temperature from 300 to 360 °K was considered in the experiments to evaluate the effect of feed temperature. As observed, the permeation flux increases by increasing feed temperature. This is because the transport mechanism in pervaporation systems using dense membranes is the solution-diffusion mechanism [47, 48]. Increasing temperature would result in enhancement of solubility and diffusivity of sulfur in the composite membrane (PVP/PU=0.2). Also, free volume in polymer structure increase with increasing temperature which makes easy transfer of molecule from one side to other side. Consequently, increasing of flux leads to higher amount of non-sulfur hydrocarbon molecules penetrate in to the permeate side which cause reduction of enrichment factor (see Fig. 5). The maximum enrichment factor is obtained at feed temperature of 300°K.

Fig. 5: Effect of temperature on mass flux and enrichment factor. Sulfur concentration in the feed =200 ppm, (PVP/PU=0.2).

3-3- Impact of PVP concentration on desulfurization

Effect of PVP concentration on the mass transfer flux and enrichment factor of sulfur is depicted in Fig. 6. PVP/PU membranes were prepared at different concentrations ranging from the PVP/PU ratio of 0-1. The amount of water in feed solution is 100 ppm which it is half of the sulfur content in the feed stream. Due to hydrophilic nature of PVP [49-51], increasing PVP content in membrane causes the water flux compared to sulfur flux increases drastically. Consequently, the enhancement of water flux results in decreasing sulfur mass flux through the membrane. In addition, adding PVP to membrane leads to the reduction of interaction between organic compounds and PVP. So, the tendency of feed which is mostly organic compounds to permeate though membrane decreases. On the other hand, enrichment factor fluctuates between 1.11 and 1.57. Finally, PVP/PU ratio of 0.2 is considered as the best PVP concentration. In addition, with increasing PVP concentration from 0 to 20 percent the amount of enrichment factor increase from 1.111 to 1.57. This can be explained by solubility parameters of typical sulfur species and PVP. Solubility parameters of PVP and sulfur species are 20.56 and 19-20 respectively. So, more sulfur compounds penetrate through membrane because more similar solubility parameters lead to the enhancement of sulfur species affinity to the composite PVP/PU membrane [52].

Fig. 6: Effect of the PVP amount on pervaporation performance.

3-4-Effect of sulfur content in the feed

Effect of sulfur content in the feed on mass transfer flux and enrichment factor are depicted in Figs. 7 and 8. The concentration of sulfur in the feed solution changes from 220 to 800 ppm at feed temperature of 298K. As it can be observed, concentration of sulfur has considerable effect on enrichment factor especially at lower feed concentrations. From Fig. 7, an increase of sulfur content in the feed results in a sharp decrease of sulfur enrichment factor. It should be pointed out that hydrocarbon compounds are normally difficult to diffuse into the non-swollen membranes while they can diffuse easily through swollen membrane. Therefore, sorption selectivity toward sulfur decreases with increasing sulfur content in the feed. From Fig. 8, it can be due to the occurrence of swelling balance in the membrane and the saturated sulfur concentration on the surface of the membrane, flux factor changes slightly with the increasing sulfur content of feed.

Fig. 7: Effect of sulfur content on enrichment factor. T= 25°C.

Fig. 8: Effect of sulfur content on permeation flux. T= 25 °C.

3-5- Effect of feed flow rate

Mass transfer flux of sulfur increases with enhancement of feed flow rate as shown in Fig. 9, due to the decrease of concentration polarization and temperature polarization. Generally, concentrations of sulfur compounds on the membrane surface which are more permeable components are lower than that in the bulk of solution. A reduction of concentration polarization means that sulfur concentration near the membrane wall was close to its amount in the bulk. The increase of sulfur concentration on the membrane surface with the feed rate enhances sulfur compounds sorption and swelling in the membrane so that results in increasing mass transfer flux. The results indicated that the operation of pervaporation system at high flow rate was more favorable.

Fig. 9: The effect of feed flow rate on mass flux.

3-6- The percentage of swelling of the membrane at different PVP/PU ratio

The percentage of swelling at various PVP/PU ratios ranging from 0 to 1 is shown in Fig. 10. According to the swelling test, the membranes are weighted every 1 hour for 5 hours. The membranes are placed in the solvent for 72 hours to ensure reaching steady state conditions. It is clearly seen that a reducing trend can be observed for swelling with increasing PVP content in the membrane. The latter could be attributed to the increasing hydrophilicity of membrane.

Fig. 10: The percentage of membrane swelling at different PVP/PU ratios.

3-7- Modeling results

3-7-1- Concentration distribution of sulfur

Sulfur concentration distribution in the feed and membrane sides is shown in Fig. 11. The concentration is exposed in dimensionless form. It can be seen that the feed solution including sulfur/gasoline enters the pervaporation system where the sulfur has a maximum concentration (C_0). Sulfur is transferred from bulk feed to the membrane wall because of the concentration difference as driving force in the feed side. The diffusion and convection are the sulfur mechanisms transfer in the feed side. The sulfur is then penetrated through the dense membrane via diffusion mechanism. Finally, sulfur is evaporated by the induced vacuum at the membrane-permeate interface. The sulfur concentration at permeate-membrane interface is assumed to be negligible because of low pressure induce via vacuum pump.

Fig. 11: Concentration distribution of sulfur in the feed and membrane compartments.

4- Conclusions

Refinery naphtha feed desulfurization of gasoline can be accomplished by pervaporation processes using a blend PU/PVP membrane. Contact angle and surface tension results revealed that adding PVP to PU membrane leads to the reduction of contact angle and surface tension which confirm hydrophilicity of synthesized mixed (PVP/PU) membranes. Permeation mass flux decreased with increasing sulfur content in feed stream while an enhancement was observed with the feed temperature increase. Sulfur enrichment factor maintained constant firstly and decreased when temperature rose. Permeation flux was shown to increase with increasing feed flow rate in the membrane module. Permeation flux was not changed while sulfur enrichment factor decreased as the feed sulfur content increased in the feed stream. Furthermore, a mathematical model was developed to simulate the separation of sulfur from sulfur/gasoline solution.

Nomenclature

A	effective area of membrane (m^2)
C_s	concentration of sulfur (mol/m^3)
$C_{s\text{-}feed}$	concentration of sulfur in the feed (mol/m^3)
$C_{s\text{-}membrane}$	concentration of sulfur in the membrane (mol/m^3)
C_0	inlet concentration of sulfur (mol/m^3)
D	diffusion coefficient (m^2/s)
F	body force (N)
J	total permeation flux (kg/m^2.h)
L	module length (m)
m	partition coefficient of sulfur between feed and membrane (-)

p	pressure (Pa)
R_E	chemical reaction (mol/m^3.s)
R	gas constant (J/mol.K)
t	time (s)
V	velocity vector (m/s)
x	axis coordinate (m)
y	axis coordinate (m)

Abbreviations

PU	polyurethane
PVP	poly vinyl chloride
PV	pervaporation
FEM	finite element method

Greek symbols

ρ	density of feed solution (kg/m^3)
μ	viscosity of feed solution (kg/m.s)

Subscripts

w	water
m	membrane
S	Sulfur

References

1. R. A. Amaral, A. C. Habert and C. P. Borges, *Materials Letters*, 2014, **137**, 468-470.
2. H. R. Mortaheb, F. Ghaemmaghami and B. Mokhtarani, *Chemical Engineering Research and Design*, 2012, **90**, 409-432.
3. T. G. Kaufmann, A. Kaldor, G. F. Stuntz, M. C. Kerby and L. L. Ansell, *Catalysis Today*, 2000, **62**, 77-90.
4. C. Song, *Catalysis Today*, 2003, **86**, 211-263.
5. R. Qi, Y. Wang, J. Chen, J. Li and S. Zhu, *Journal of Membrane Science*, 2007, **295**, 114-120.
6. F. L. Plantenga and R. G. Leliveld, *Applied Catalysis A: General*, 2003, **248**, 1-7.
7. M. F. Ali, A. Al-Malki, B. El-Ali, G. Martinie and M. N. Siddiqui, *Fuel*, 2006, **85**, 1354-1363.
8. M. Rezakazemi, K. Shahidi and T. Mohammadi, *International Journal of Hydrogen Energy*, 2012, **37**, 17275-17284.
9. M. Rezakazemi, K. Shahidi and T. Mohammadi, *International Journal of Hydrogen Energy*, 2012, **37**, 14576-14589.
10. M. Rostamizadeh, M. Rezakazemi, K. Shahidi and T. Mohammadi, *International Journal of Hydrogen Energy*, 2013, **38**, 1128-1135.
11. *U.S. Pat.,* 0211706 A1, 2004.
12. E. Ito and J. A. R. van Veen, *Catalysis Today*, 2006, **116**, 446-460.
13. J. Chen, J. Li, R. Qi, H. Ye and C. Chen, *Journal of Membrane Science*, 2008, **322**, 113-121.
14. B. Li, S. Yu, Z. Jiang, W. Liu, R. Cao and H. Wu, *Journal of Hazardous Materials*, 2012, **211–212**, 296-303.

15. L. Lin, Y. Kong, K. Xie, F. Lu, R. Liu, L. Guo, S. Shao, J. Yang, D. Shi and Y. Zhang, *Separation and Purification Technology*, 2008, **61**, 293-300.
16. L. Lin, Y. Kong and Y. Zhang, *Journal of Membrane Science*, 2008, **325**, 438-445.
17. *U.S. Pat.,* 0026321 A1, 2004.
18. I. G. Wenten, *Membrane Science and Technology*, 2002, **24**, 1009-1024.
19. L. Lin, G. Wang, H. Qu, J. Yang, Y. Wang, D. Shi and Y. Kong, *Journal of Membrane Science*, 2006, **280**, 651-658.
20. L. Lin, Y. Kong, J. Yang, D. Shi, K. Xie and Y. Zhang, *Journal of Membrane Science*, 2007, **298**, 1-13.
21. L. Lin, Y. Zhang and Y. Kong, *Fuel*, 2009, **88**, 1799-1809.
22. Y. K. Fu Wei Lu, Hong Ling Lv, Jun Ding and Jin Rong Yang, *Advanced Materials Research*, 2011, **150-151**, 317-320.
23. Z.-J. Yang, Z.-Q. Wang, J. Li and J.-X. Chen, *Separation and Purification Technology*, 2013, **109**, 48-54.
24. R. Qi, Y. Wang, J. Chen, J. Li and S. Zhu, *Separation and Purification Technology*, 2007, **57**, 170-175.
25. R. Cao, X. Zhang, H. Wu, J. Wang, X. Liu and Z. Jiang, *Journal of Hazardous Materials*, 2011, **187**, 324-332.
26. M. Jain, D. Attarde and S. K. Gupta, *Journal of Membrane Science*, 2015, **490**, 328-345.
27. Z. Yang, W. Zhang, J. Li and J. Chen, *Separation and Purification Technology*, 2012, **93**, 15-24.
28. L. Lin, Y. Kong, G. Wang, H. Qu, J. Yang and D. Shi, *Journal of Membrane Science*, 2006, **285**, 144-151.

29. R. Xu, G. Liu, X. Dong, Wanqin and Jin, *Desalination*, 2010, **258**, 106-111.

30. Z. Yang, T. Wang, X. Zhan, J. Li and J. Chen, *Industrial & Engineering Chemistry Research*, 2013, **52**, 13801-13809.

31. M. Ghadiri and S. N. Ashrafizadeh, *Chemical Engineering & Technology*, 2014, **37**, 597-604.

32. M. Rezakazemi, A. Ghafarinazari, S. Shirazian and A. Khoshsima, *Polymer Engineering & Science*, 2013, **53**, 1272-1278.

33. S. Shirazian, A. Marjani and M. Rezakazemi, *Engineering with Computers*, 2012, **28**, 189-198.

34. M. Fasihi, S. Shirazian, A. Marjani and M. Rezakazemi, *Mathematical and Computer Modelling*, 2012, **56**, 278-286.

35. R. B. Bird, W. E. Stewart and E. N. Lightfoot, *Transport Phenomena*, John Wiley & Sons, New York, 2en ed. edn., 2002.

36. M. Ghadiri, M. Parvini and M. G. Darehnaei, *Polymer Engineering & Science*, 2014, **54**, 2222-2227.

37. K. Tahvildari, A. Zarabpour, M. Ghadiri and A. Hemmati, *Polymer Engineering & Science*, 2014, **54**, 2553-2559.

38. F. Barati, M. Ghadiri, R. Ghasemi and H. M. Nobari, *Chemical Engineering & Technology*, 2014, **37**, 81-86.

39. M. Ghadiri, V. Abkhiz, M. Parvini and A. Marjani, *Chemical Engineering & Technology*, 2014, **37**, 543-550.

40. M. Ghadiri, S. Fakhri and S. Shirazian, *Polymer Engineering & Science*, 2014, **54**, 660-666.

41. M. Ghadiri, M. Ghasemi Darehnaei, S. Sabbaghian and S. Shirazian, *Chemical Engineering & Technology*, 2013, **36**, 507-512.

42. M. Ghadiri, A. Marjani and S. Shirazian, *International Journal of Greenhouse Gas Control*, 2013, **13**, 1-8.

43. M. Ghadiri and S. Shirazian, *Chemical Engineering and Processing: Process Intensification*, 2013, **69**, 57-62.

44. S. A. Miramini, S. M. R. Razavi, M. Ghadiri, S. Z. Mahdavi and S. Moradi, *Chemical Engineering and Processing: Process Intensification*, 2013, **72**, 130-136.

45. F. Nosratinia, M. Ghadiri and H. Ghahremani, *Journal of Industrial and Engineering Chemistry*, 2014, **20**, 2958-2963.

46. J. Zhu, Y. Zhang, M. Tian and J. Liu, *ACS Sustainable Chemistry & Engineering*, 2015, **3**, 690-701.

47. A. Wolińska-Grabczyk, *Journal of Membrane Science*, 2006, **282**, 225-236.

48. V. S. Cunha, M. L. L. Paredes, C. P. Borges, A. C. Habert and R. Nobrega, *Journal of Membrane Science*, 2002, **206**, 277-290.

49. G. O. K. Loh, Y. T. F. Tan and K. K. Peh, *Powder Technology*, 2014, **256**, 462-469.

50. E.-J. Kim, M.-K. Chun, J.-S. Jang, I.-H. Lee, K.-R. Lee and H.-K. Choi, *European Journal of Pharmaceutics and Biopharmaceutics*, 2006, **64**, 200-205.

51. M. Moneghini, A. Carcano, G. Zingone and B. Perissutti, *International Journal of Pharmaceutics*, 1998, **175**, 177-183.

52. K. Liu, C.-J. Fang, Z.-Q. Li and M. Young, *Journal of Membrane Science*, 2014, **451**, 24-31.

Figure Captions:

Fig. 1: Experimental setup used for pervaporation desulphurization of gasoline.

Fig. 2: Model domain used in the simulation.

Fig. 3: SEM images of synthesized composite membranes at different PVP loadings. a: pure PU; b: PVP/PU=0.2; c: PVP/PU=0.4; d: PVP/PU=0.6; e: PVP/PU=0.8; f: PVP/PU=1.

Fig 4: Contact angles of 0% PVP, 40% PVP, 80% PVP.

Fig. 5: Effect of temperature on mass flux and enrichment factor. Sulfur concentration in the feed =200 ppm, (PVP/PU=0.2).

Fig. 6: effect of the PVP amount on pervaporation performance.

Fig. 7: Effect of sulfur concentration on enrichment factor. T= 25°C.

Fig. 8: Effect of sulfur concentration on permeation flux. T= 25 °C.

Fig. 9: The effect of feed flow rate on mass flux.

Fig. 10: The percentage of membrane swelling at different PVP/PU ratios.

Fig. 11: Concentration distribution of sulfur in the feed and membrane compartments.

Table captions:

Table 1: Boundary conditions for momentum and mass transfer equations

Table 2: Surface tension of 0% PVP, 40% PVP, 80% PVP.

Fig. 1:

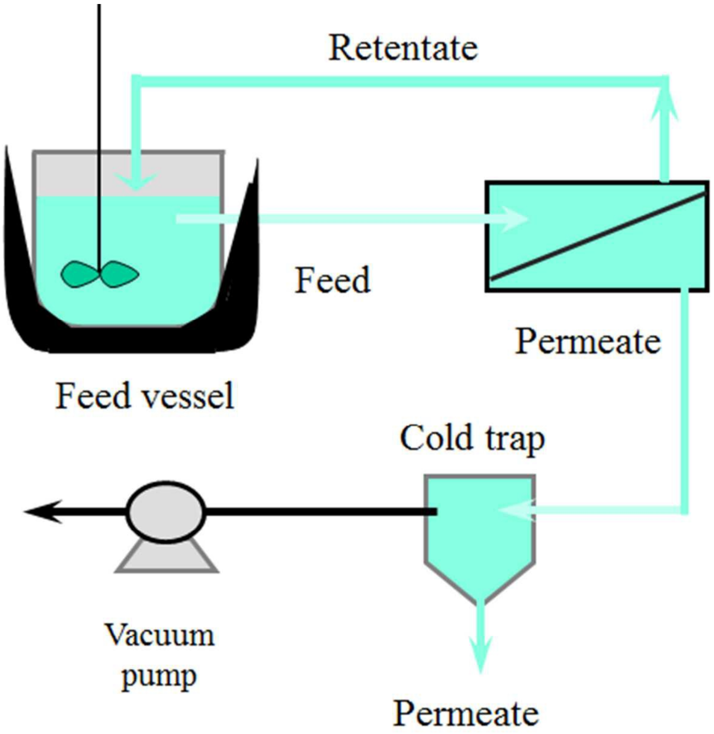
Retentate
Feed
Permeate
Feed vessel
Cold trap
Vacuum pump
Permeate

Fig. 2:

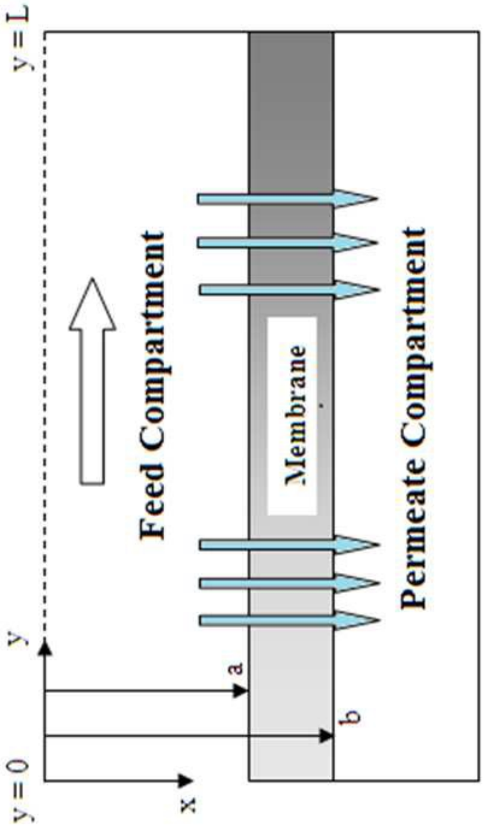
y = L
y = 0
y
x
a
b
Feed Compartment
Membrane
Permeate Compartment

Fig. 3:

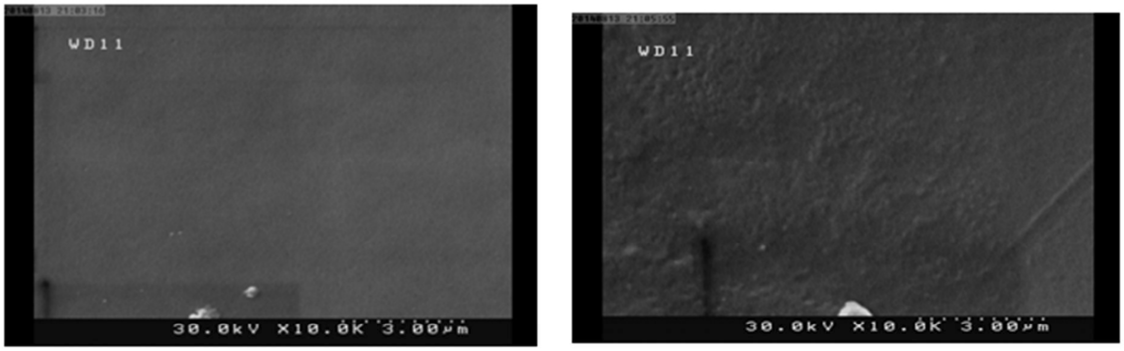

(a, PVP/PU=0)

(b, PVP/PU=0.2)

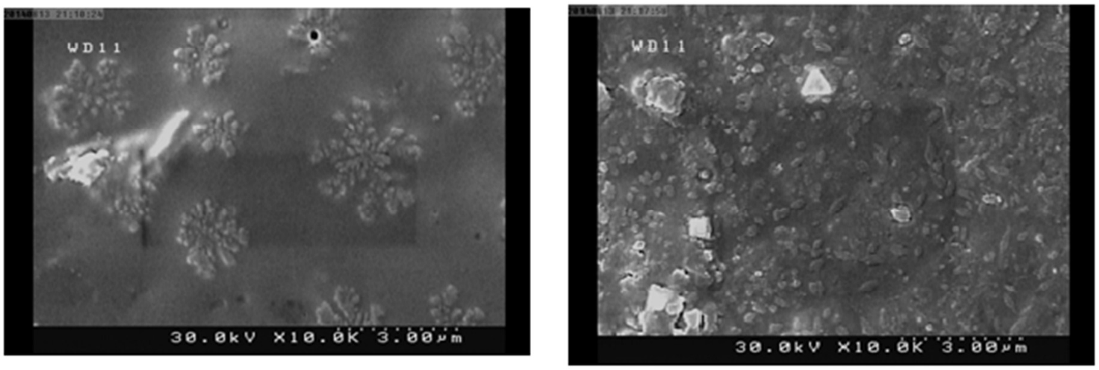

(c, PVP/PU=0.4)

(d, PVP/PU=0.6)

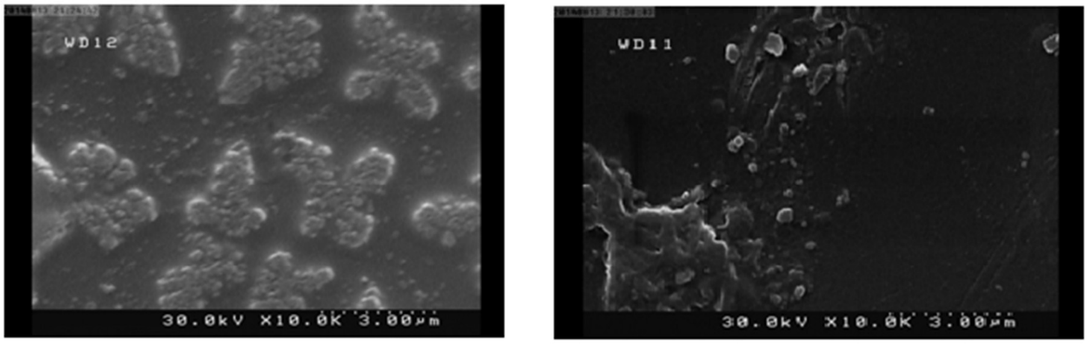

(e, PVP/PU=0.8)

(f, PVP/PU=1)

Fig. 4:

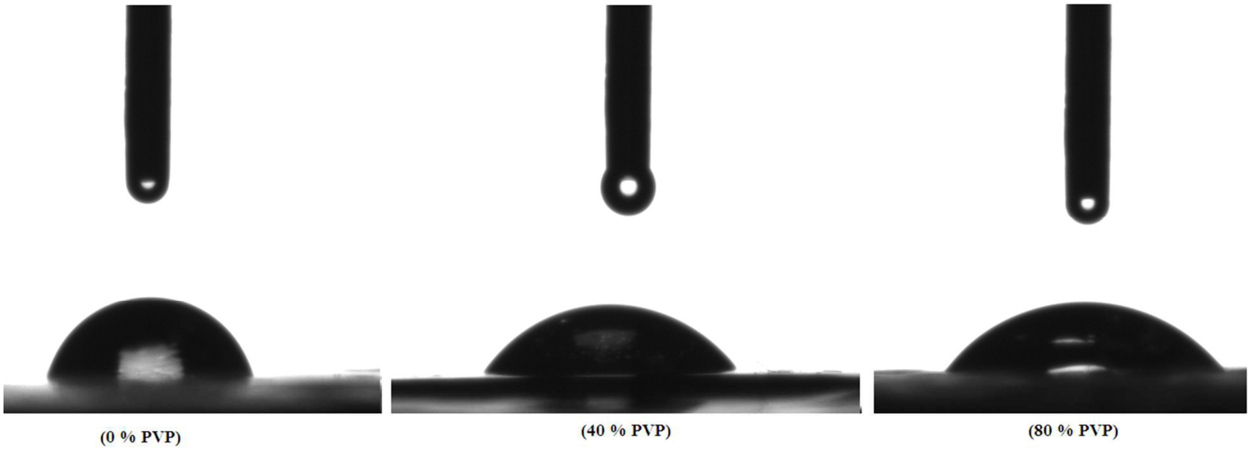
(0 % PVP) (40 % PVP) (80 % PVP)

Fig. 5:

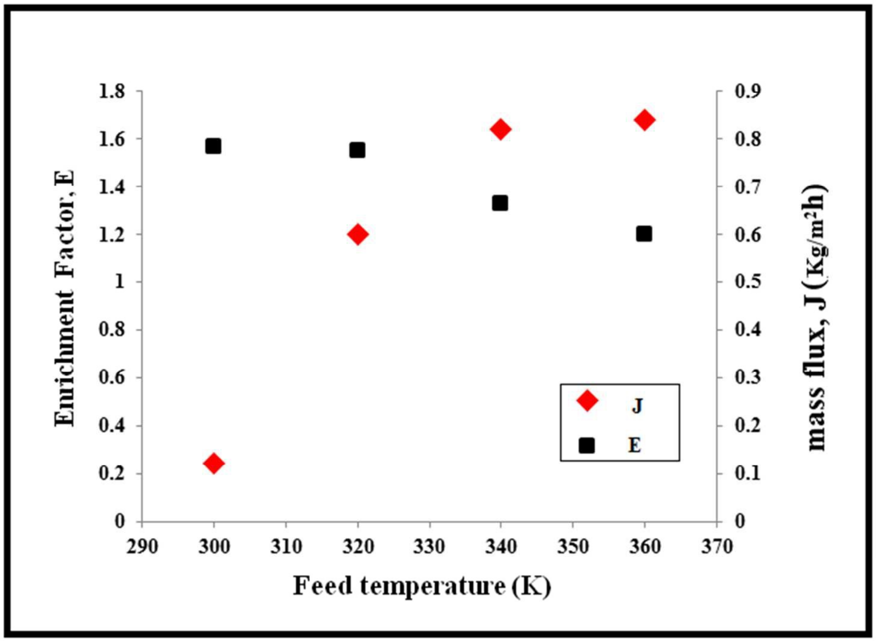
Enrichment Factor, E
mass flux, J (Kg/m²h)
Feed temperature (K)
1.8
1.6
1.4
1.2
1
0.8
0.6
0.4
0.2
0
0.9
0.8
0.7
0.6
0.5
0.4
0.3
0.2
0.1
0
290
300
310
320
330
340
350
360
370
J
E

Fig. 6:

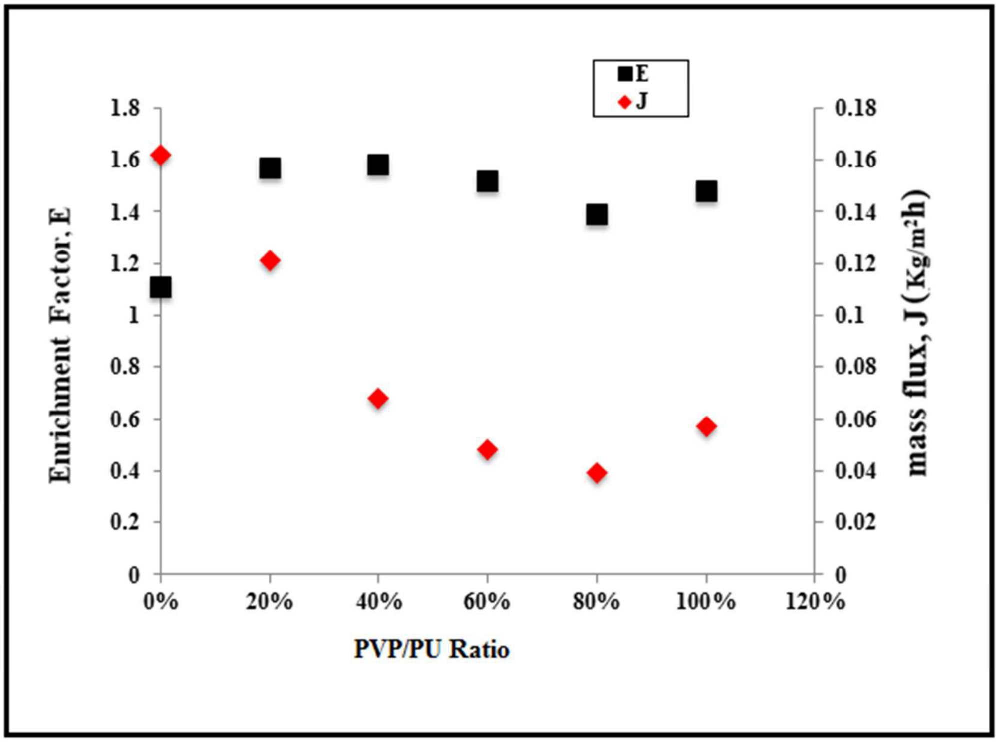
■ E
◆ J
Enrichment Factor, E
mass flux, J (Kg/m²h)
1.8
1.6
1.4
1.2
1
0.8
0.6
0.4
0.2
0
0.18
0.16
0.14
0.12
0.1
0.08
0.06
0.04
0.02
0
0%
20%
40%
60%
80%
100%
120%
PVP/PU Ratio

Fig. 7:

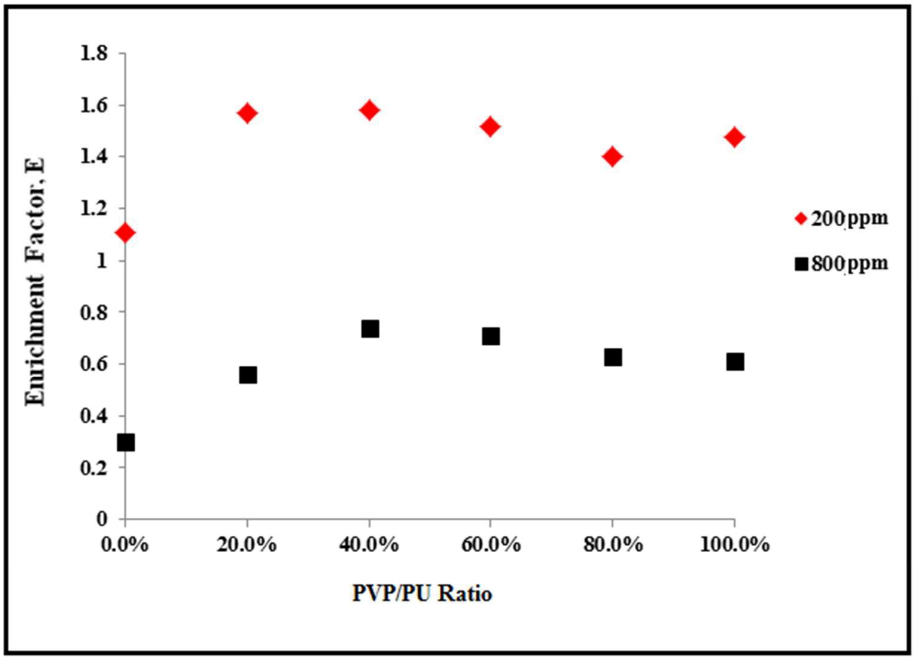
Enrichment Factor, E
1.8
1.6
1.4
1.2
1
0.8
0.6
0.4
0.2
0
0.0%
20.0%
40.0%
60.0%
80.0%
100.0%
PVP/PU Ratio
◆ 200 ppm
■ 800 ppm

Fig. 8:

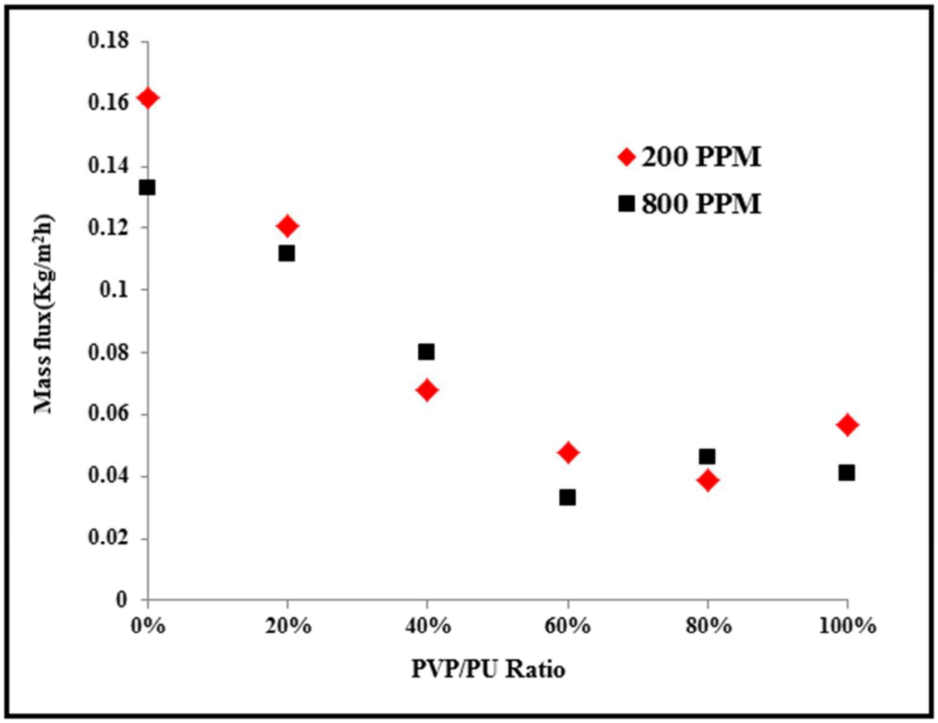
0.18
0.16
0.14
0.12
0.1
0.08
0.06
0.04
0.02
0
Mass flux(Kg/m²h)
0%
20%
40%
60%
80%
100%
PVP/PU Ratio
◆ 200 PPM
■ 800 PPM

Fig. 9:

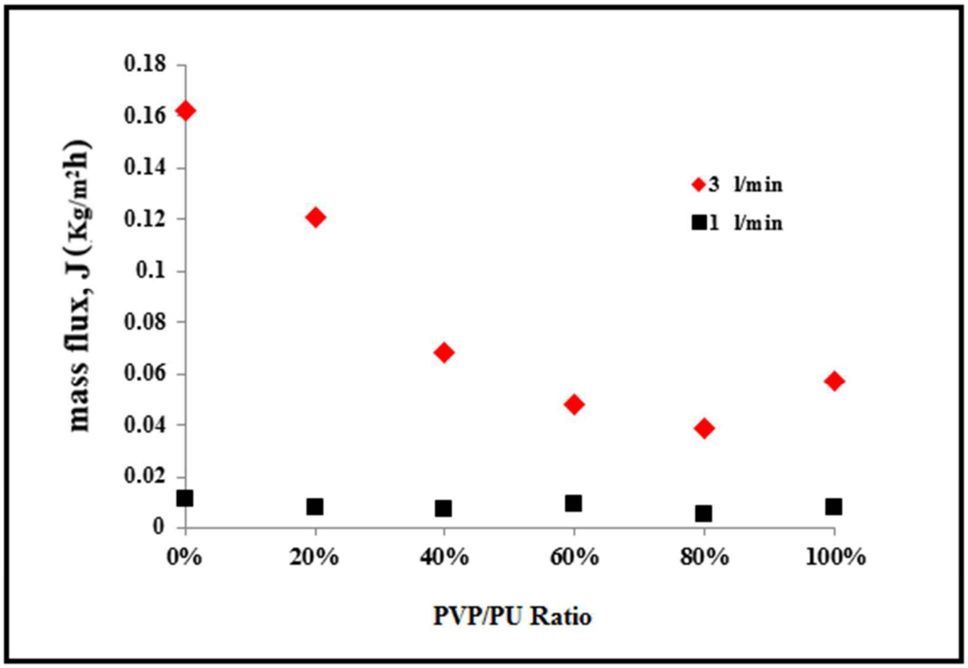
mass flux, J (Kg/m²h)
0.18
0.16
0.14
0.12
0.1
0.08
0.06
0.04
0.02
0
◆3 l/min
■1 l/min
0%
20%
40%
60%
80%
100%
PVP/PU Ratio

Fig. 10:

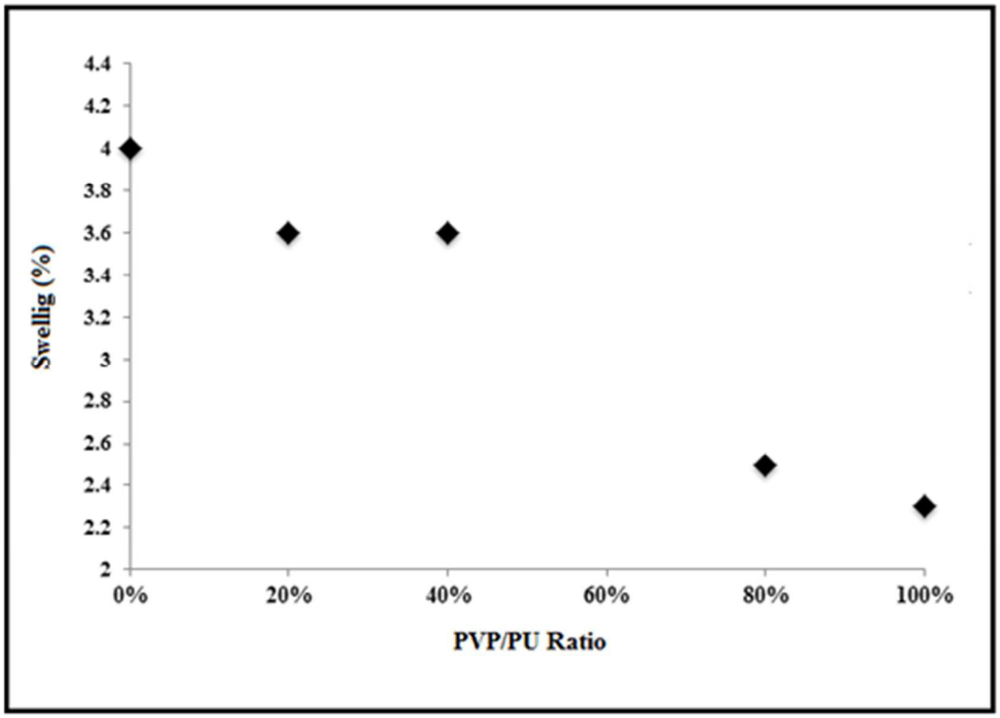
Swellig (%)
4.4
4.2
4
3.8
3.6
3.4
3.2
3
2.8
2.6
2.4
2.2
2
0%
20%
40%
60%
80%
100%
PVP/PU Ratio

Fig. 11:

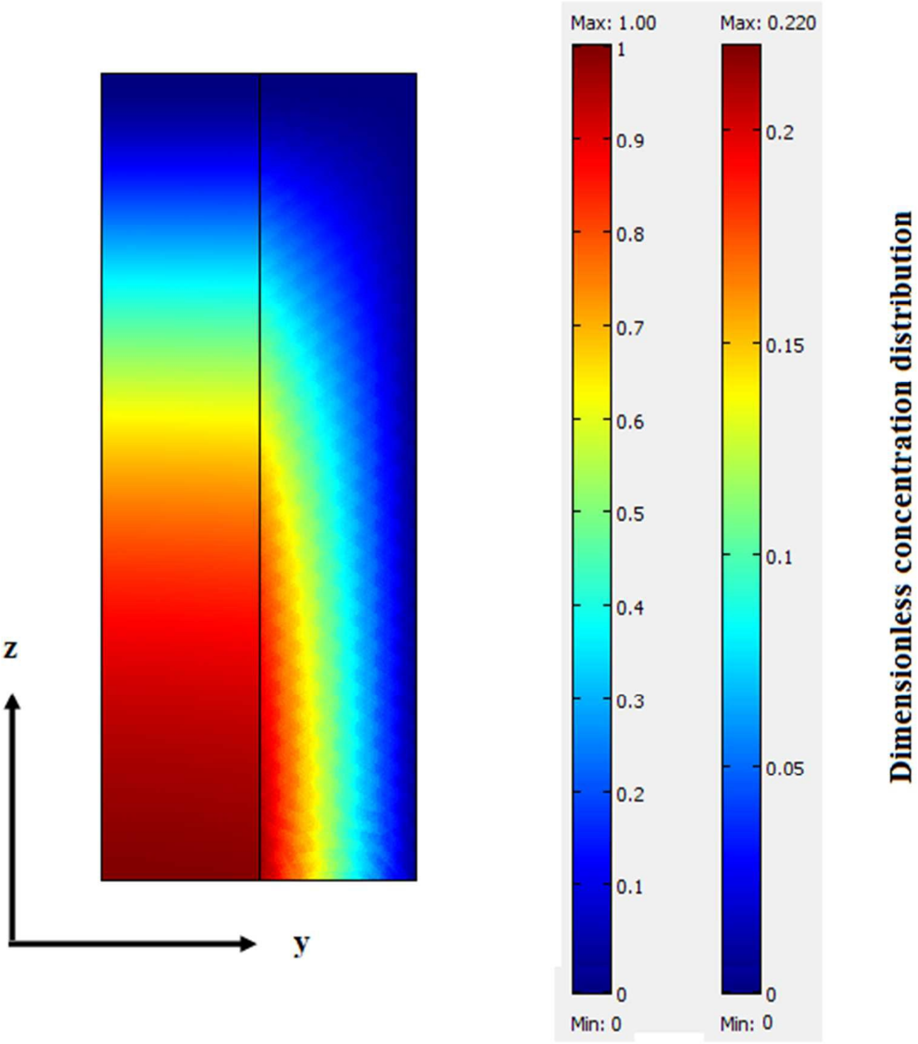
z
y
Max: 1.00
1
0.9
0.8
0.7
0.6
0.5
0.4
0.3
0.2
0.1
0
Min: 0
Max: 0.220
0.2
0.15
0.1
0.05
0
Min: 0
Dimensionless concentration distribution

Table 1:

Position	Feed side (Mass)	Feed side (Momentum)	Membrane (Mass)
y=0	Cs-feed=C_0	$V_y=V_0$	$\frac{\partial C_{s-membrane}}{\partial y}=0$
y=L	$\frac{\partial C_{s-feed}}{\partial y}=0$	$V_y=0$	$\frac{\partial C_{s-membrane}}{\partial y}=0$
x=0	Convective flux	$p=p_{atm}$	-
x=a	$C_{s\text{-}feed}=C_{s\text{-}membrane}/m$	$V_y=0$	$C_{s\text{-}membrane}=C_{s\text{-}feed} \times m$
x=b	-	-	$C_{s\text{-}membrane}=P/RT$

Table 2:

Sample	Surface tension	Unit
0% PVP	77.1	(mN/m)
40% PVP	55.6	(mN/m)
80% PVP	51.1	(mN/m)